Multihole gasoline direct injection spray plumes

R. Rotondi[a], J. Hélie[b] , C. Leger[c], M. Mojtabi[d] and G. Wigley[d],
[a] Continental Automotive Gmbh
Siemensstrasse 12, 93055 Regensburg, Germany
[b]Continental Automotive SAS
1 Avenue Paul Ourliac – BP 1149 Toulouse Cedex 1, France
[c] Continental Automotive Italy
Via Livornese 1319, San Piero a Grado, PI
[d] Loughborough University, Department of Aeronautical and Automotive Engineering,
Stewart Miller Building, West Park, Leicestershire
LE11 3TU, United Kingdom

Corresponding author : jerome.helie@continental-corporation.com

Abstract

GDI multi-hole injector spray dynamics are investigated numerically and experimentally to determine the secondary atomization regimes and jet to jet interactions. Parameters which affect the global penetration are analysed and local velocity and droplet size fields are obtained from the experimental and numerical results to illustrate the spray structures.

Introduction

In Gasoline Direct Injection engines, spray penetration has to be reduced to a minimum to limit fuel impact on in-cylinder surfaces which lead to soot when piston or valve are impacted and oil dilution when the cylinder wall is impacted. Multi-hole gasoline injectors produce spray plumes which exhibit a high exit velocity (up to 150-180m/s at 200bar) with a large spray plume angle (usually from 8 to 18deg). With their flexibility in the choice of spray plume orientation, they offer an interesting alternative to single-hole pressure swirl and piezoelectric injectors. The quality of the mixture preparation is linked to the targeting (plume orientation) and the ability of the spray to evaporate quickly at a defined location. The evaporated spray can be homogenized by the air movement to limit the HC and Particles Number emissions and provide high engine efficiency. These design guidelines will become of higher importance as the engine downsizing trend continues. Additionally, for high BMEP engines, avoiding spurious auto-ignition (rumble or knock) is another important topic linked to the quality of mixture (vapor, temperature) homogeneity..

We focus in the present paper on the atomization performance of GDI multi-hole injectors. Such injectors operate in a pressure range higher than the port fuel injectors operating pressure range and lower than Diesel injectors. Their hole length-to-diameter ratio is quite small (typically from 0.5 to 2). The primary atomization, not developed in detail here (see the twin paper [1] for further details), remains a very important part of atomization process for these atomizers, as cavitation is involved [2]. The interesting features of the multi-hole injector are the overall stability of the spray angle when the in-cylinder pressure varies and the possibility to select the jet directions to avoid impacts and improve the mixture formation. However, the spatial targeting cannot be chosen arbitrarily by only considering the final mixture quality results. For small total spray angles, dependent on the hole-to-hole distance and jet direction, the spray is affected by jet-to-jet interaction [3]. For low in-cylinder pressure, corresponding to low-to-medium engine load (2 to 5bar BMEP), the existing liquid phase can undergo "flash boiling", i.e. the liquid fuel reaches the vapour phase limit through the pressure decrease in the nozzle [4]. Such behaviour is enhanced by the vapour pressure dependency on temperature and hot engine operating conditions, by a low injection rate and by any stop-and-start strategies.

In the present paper we limit our study to the non-critical injection conditions and focus on the single jet formation with and without strong evaporation, and the jet-to-jet interaction in atmospheric conditions. Conventional break-up and spray model results are compared to penetration and angle measurements determined by spray imaging performed in a constant volume vessel under different pressure and temperature conditions and to

PDA measurements obtained under atmospheric conditions. We focus especially on the secondary break-up process which is not very detailed in the current literature on GDI multi-stream (MSI) injectors.

The injectors considered for the study are Continental Multi-Stream (MSI) XL2 with 6 holes in a symmetrical pattern a hole length-to-diameter ratio of unity and with operational fuel pressures up to 200bar. Two different injectors were used, one with a nominal external cone angle (CA) of 60° and a static flow rate of 18mm^3/s at 120bar and the other with a nominal external cone angle of 90° and a static flow rate of 12mm^3/s at 120bar. The 60°CA injector was tested at 120 and 200bar and the 90°CA injector at 120 and 180bar. Regular RON-95 gasoline was used.

Numerical & experimental tools

The gaseous flow is represented by the average (RANS) approach. The droplet modelling is based on a Lagrangian approach with the Particle In Cell technique, where stochastic dispersion is used [5]. The Evaporation model used is from Abramzon [6], as implemented in the FIRE-AVL solver. The incompressible solver used is the SIMPLE algorithm with 20000 blobs per hole within a grid of 1mm size. Later in the paper, the validity of the conventional spray break-up models is discussed.

The first series of measurements involved simultaneous imaging and PDA. For the imaging study a Xenon flash unit was the light source. This was coupled to a Fostec fibre optic panel to provide a uniform background light intensity distribution against which the nozzle and spray was imaged. The time corresponding to maximum intensity was used as the trigger to activate the camera with its exposure time set to 0.5 μs. The main aim of the imaging work was to quantify the spray cone angle and penetration.

Single-shot images were digitally recorded with a PCO Sensicam Fast Shutter CCD camera equipped with a Nikon 55 mm focal length macro lens. The focal plane for the lens was the axis of the injector body and the vertical plane through the input laser beams of the PDA system. The camera provided an image size of approximately 50 by 40 mm, represented by 1280 by 1024 pixels, with an intensity level resolution of up to 12 bits.

The injector control unit provided an electronic trigger, referenced to the opening pulse of the injector solenoid, which, through a variable delay unit, controlled both the flash and image capture time. Twenty images were stored for each time delay to allow, an evaluation of shot to shot variations and a mean image to be created to highlight bulk features.

The design, construction and application of the two component PDA transmission system to GDI fuel sprays has been well documented [7]. The configuration for the 488 and 514 nm laser beam wavelengths at the final focusing lens was: beam diameters of 5 mm, equal beam pair separations of 50 mm, laser powers of 100 and 200 milli-watts per beam, and with a focal length of 300 mm produced coincident measurement volumes of diameters of 56 and 59 microns with fringe spacing of 3.10 and 2.94 microns respectively for the two wavelengths. This produced an experimental velocity bandwidth of nominally -30 to 110 m/s.

The standard Dantec 57X10 receiver optical system was positioned at a scattering angle of 70 degrees with the aperture micrometer setting set to 0.5 mm. This optical configuration resulted in an effective measurement volume length of 0.1 mm and a maximum drop size measurement range of up to 100 microns. At each measurement position 100,000 validated data samples were attempted or an elapsed time of 50 seconds was reached i.e. 250 injections. This first experiment type will be referred to as the "atmospheric free" data.

A second series of measurements were performed. The injectors were fitted into a constant volume chamber with an internal volume of X diameter by Y mm with three windows for straight through and orthogonal optical access. The pressure inside the chamber could be varied from 0.1bar to 10bar. A vacuum pump was used to achieve the sub atmospheric pressure range while a nitrogen cylinder was used to pressurize the chamber up to 10bar. The chamber had two electrically-actuated valves, an inlet valve linked to the pressure release valve of a nitrogen cylinder and an outlet valve linked to a vacuum pump which was connected to an exhaust extractor. A pressure sensor monitored the pressure inside the chamber.

The chamber is insulated and mounted on top of a heating plate with a temperature control and an operating range between 20°C and 100°C. Considering the low injection repetition rate of 1Hz and the low fuel quantity injected during the 0.8ms injection duration, nominally 10 and 7 mg per shot for the 60° and 90° injectors respectively, it was assumed that conductive heat transfer through the injector was the main physical process affecting the temperature of the fuel injected into the chamber. Hence injector temperature was equal to the temperature of the chamber. A thermocouple measured the temperature of the gas in the chamber and displayed this information on a control interface and which was also used to determine the required power to the heating plate.

The experimental setup and its application are detailed in [4]. The same Mie imaging technique, using a similar CCD camera and xenon flash as described above, was performed to record images of the spray at various temperatures and sub-atmospheric pressures. Such second experiment type will be referred to as the "slow evaporating" data.

The last type of measurement was obtained by mounting similar multi-stream injectors in a hot and counter-pressured environment inside the ESYTEC-LTT Erlangen GDI Chamber [8,9]. These measurements will be referred to as the "highly evaporating" data.

Single jet propagation and secondary break-up mechanism

In the present study blobs are injected at the injector outlet, with the experimentally determined spray angle considered as an input. The droplets formed after the disintegration of the liquid jet may undergo secondary breakup. Because of the forces acting on a droplet, as it moves in the surrounding gas, a non-uniform pressure distribution is developed around it. This process leads to droplet deformation and subsequent break-up. The relevant forces involved in this physical phenomenon are those related to surface tension, viscosity, inertia and surface instabilities responsible for wave growth. Rayleigh-Taylor (R-T) instabilities may occur at drop windward surface when a body force is directed normally to the interface of the two fluids from the dense to the less dense one. Kelvin-Helmholtz (K-H) instabilities are due to the shear forces in the relative parallel motion at the common interface. Different regimes can be observed as the relative magnitude of these forces varies. One possible classification can be made over different ranges of droplet Weber number, *We*:

$$We = \frac{\rho_l U^2 D}{\sigma_l} \tag{1}$$

where U is the velocity, D the diameter, ρ_l the liquid density and σ_l the surface tension.

We=12: Vibrational mode - Fragmentation is caused by the amplification of droplet deformation originated by vibrational resonance of liquid surface;

12<We<45: Bag regime - Drop break-up is due to the deformation of the droplet in a bag-like structure that disintegrates once a critical value of deformation is reached (figure 1);

45<We<100: Chaotic regime - A transitional regime in which droplet break-up is due to both ballooning and breaking of filaments resulting from the liquid surface layer ripping;

100<We<1000: Stripping regime - The flow over the drop causes the ripping of the surface inducing a thin laminar boundary on it. After a certain stage of deformation, the boundary layer is stripped from the periphery because of K-H instabilities effects, in the form of films and fragments (Boundary Layer Stripping). Drop diameter gradually reduces and, when a critical value is reached, the drop disintegrates in smaller ones with bimodal distribution (figure 2);

We>1000: Catastrophic regime - At very high Weber number both R-T and K-H instabilities are involved. The former, due to droplet deceleration and related with higher values of wavelength and amplitude, lead to the formation of bigger drops then those related with K-H instabilities associated with lower values of wavelength and amplitude (figure 3).

For the medium range of injection pressures typical of GDI homogeneous combustion systems no Catastrophic regime is observed. This is contradictory to what previous authors [3,10] found for GDI application. Dahlender [3] used iso-octane with 10% of 3-pentanone, 250bar/10bar fuel/air pressure respectively but with a Diesel injector with length-over-diameter ratio of 10 which can influence the primary break-up process significantly and leads to small plume angles. These conditions are at the lower limit of the catastrophic regime. In Esmail [10] the value of L-over-D is not mentioned, but the operating conditions are lower (fuel pressure 30bar to 100bar and ambient air pressure), while the fluid used was a dry-solvent.

The well known TAB model is based on the analogy between an oscillating droplet and a spring-mass system. The break-up is due to the amplification of droplet deformation resulting from vibrational resonance of the surface and therefore was chosen to model droplet breakup in the vibrational regime. The Wave model considers K-H instability effects and can be used to simulate the secondary break-up in those regimes in which it may be ascribed to the shear forces at the interface. It was chosen to model the secondary break-up in the Stripping regime. The transitional Weber number was chosen to be equal to 12, therefore, droplets with a Weber number smaller than 12 were processed using the Tab model, and the ones with a Weber number greater than 12 were processed using the Wave model.

Different cases have been studied varying fuel pressure, counter pressure and fuel/vessel temperature, the maximum range of Weber number of each case varying from 40 to 350. During their lifetime drops may decelerate, break-up, evaporate and a wide range of droplet Weber number can be obtained, therefore, different secondary break-up mechanisms can occur simultaneously. In figure 2, the droplet Weber number distribution with a log-scale is shown for two different cases, a low Weber number case (120bar FUP, 1bar counter pressure) and a

high Weber number case (120bar FUP, 8bar counter pressure) at 0.6 ms, for the 90°CA injector. It can be observed that after a certain time (0.6ms in this plot), even the case with higher Weber number presents many droplets that break-up in the vibrational mode ($We \leq 12$). Therefore while during the initial life of the droplet, it will undergo mainly stripping break-up (wave), later the reduced Weber number will determine further break-up in the vibrational regime (Figure 3).

The effect on the penetration can be observed in figure 4 when comparing the experimental axial penetration to the numerical one obtained with the Wave model and with the hybrid model. After 0.6 ms the Wave model alone overestimates the penetration because all the existing droplets are processed by the Wave model while figure 2 shows that there are many droplets (note the log-scale) that have a lower Weber number, and therefore, should be processed by the Tab model which gives typically shorter break-up times.

Results compared to experimental data and jet-to-jet interaction

The penetration is well numerically reproduced in both the slow evaporating (Figure 5) and fully evaporating (Figure 6) cases. The effect of fuel pressure on the penetration is not negligible when increasing pressure from 50bar to 100 or 150bar. This effect becomes less effective with further pressure increase. Evaporating hot conditions increase the difference. The result is consistent but higher values were presented in the work of Nauwerk [11] and other authors, at least with surrounding pressures lower than 10bar [9,11]. The droplet size is slightly overestimated in ambient conditions (Figure 7). Such effect is expected due to the fact that primary break-up is not considered, which affects the simulation quality, especially for counter-pressures lower than 2bar.

Jet-to-Jet interaction is a complex phenomena appearing when the injector has a large number of holes or a small spray angle which has to be understood in detail for multi-hole injector design. Such effect can lead to partial or even full collapse of the multi jet spray under certain in-cylinder conditions.

The radial velocities for adjacent jets at 40mm below each injector nozzle at a radius corresponding to the maximum axial velocity (jet centreline) and at 2.5ms after the start of injection are given in Figure 8 (top graph). The angle 243^0 on the graph corresponds to the central jet in each case. The droplet velocity profiles for the adjacent jets are consistent on either side, however, small differences in velocities can be expected due to small variations in plume angle. The droplet velocity profiles for the 90°CA injector show evidence of three distinct jets with high velocity gradients across them but with no data between them due to a drastic reduction in droplet number between jets. The 60°CA injector obviously produces lower radial velocities due to the smaller cone angle and explains why the profile shows three complete jets within the angular range. However, the velocity profile is continuous between the three jets with significant numbers of droplets being detected. This is not seen as hole-to-hole differences but indicates strong jet to jet interactions and that these may be linked to jet-to-jet instabilities.

In the bottom plot of Figure 8 axial velocity profiles are shown from the CFD simulation and the PDA measurements for two adjacent jets for the 90°CA injector in the plane 20mm below the nozzle. Although the results are consistent from plume to plume, there are some cases which show deviations between the numerical and experimental, with a larger velocity found with the simulation across the jet center area. Skogsberg [12], reported a good agreement between PDA distributions and simulations, with velocity distributions more homogeneous with CFD than with the PDA measures [12, 10].

The conclusions on the jet-to-jet interactions in the case where the jet direction is influenced and the jets deviate from the initial targeting are as follows:- 1) The dominate physical process is air entrainment where the drag generated influences the adjacent jets making them deviate, as in a co-flow. 2) The restricted spacing between jets does not allow the development of a normal recirculation where the centrifugal force would be balanced by the pressure decrease at the center. 3) With jet-to-jet interactions, the pressure between the jets decreases allowing these zones to be filled by small droplets. Jet-to-jet interaction obviously changes with atomization, evaporation and drag, i.e. with the surrounding engine operating conditions. Surprisingly, such effects are not documented in the literature while it is a very important effect to be avoided in production development. Jet to jet interactions are qualitatively illustrated by comparing the CFD simulation and spray imaging under atmospheric conditions, figure 9, which shows excellent agreement for the latest generation XL3 60°CA injector.

Conclusion and future work

A limitation of the present CFD approach was to neglect the detailed primary atomisation. The results obtained could suggest that the primary atomisation influence the spray more on the exit angle and droplet-blobs dispersion than on the droplet size and spray velocity; however, the reader should take such an assumption cautiously. The next step will be to couple internal flow simulation with the dispersed spray simulation and to integrate progressively the results from the break-up simulation and modelling activity previously reported in [1].

Some authors did measurements of GDI Multihole spray with different fuel types. Through this, it can be possible to check the change in the break-up and in the droplet evaporating, as was done successfully for the previous generation gasoline swirl injectors [16]. Some authors found a little effect on the break-up and a large effect on the evaporation [17] whereas others found recently a strong effect on the atomizing spray development itself [18]. Our numerical work will be continued on the break-up mechanism as it can be influenced by the fluid properties.

Acknowledgments

The work has been partly realised in the framework of the French Public projects PREDIT "JETIDE2", FUI "MAGIE" (MOVEO competitive cluster) and UK program "HOTFIRE". The authors thanks Dr Zigan & Prof Wensing for the experimental measures done with ESYTEC-LTT Erlangen chamber.

References

[1] J. Shi, J. Helie, J. Cousin, ILASS-Europe, Brno, 2010.
[2] Papoulias D., Giannadakis E., Mitroglou N., Gavaises M., Theodorakakos A., SAE Paper 2007-01-1418, 2007
[3] Dahlander P., Lindgren, R., SAE paper 2008-01-0136, 2008
[4] Mojtabi M., Wigley G.and Helie, J., ILASS-Europe, Como, 2008
[5] Gosman A.D. and Ioannides, E., AIAA, 81-323
[6] Abramzon, B. and Sirignano, W. A., AIAA 26th Aerospace Sciences Meeting, 1988
[7] Wigley G., Hargrave G., and Heath J., Particle & Particle Systems Characterization, vol. 1, 1999.
[8] ESYTEC: Spray characterization of a Piezo and a solenoid GDI-Injector for gasoline and E85 operation using the Mie-scattering technique, report, 2007
[9] Koch and Leipertz, paper 06-225, ICLASS Kyoto, Japan, 2006
[10] M. Esmail, N. Kawahara, E. Tomita, M.Sumida, ICLASS 2009, Colorado USA, July 2009
[11] A. Nauwerck, J. Pfeil, A.Velji, U. Spicher, SAE 2005-01-0098, 2005
[12] M. Skogsberg, P. Dahlander, R. Lindgren and I. Denbratt, , SAE 2005-01-0097
[13] Kawara, N., Tomita E., Nakasuji, H., Sumida, M., paper 06-186, ICLASS Kyoto, Japan, 2006
[14]Xin Liu, Kyoung-Su Im, Yujie Wang and Jin Wang David L.S. Hung and James R. Winkelman Mark W. Tate, Alper Ercan, Lucas J. Koerner, Thomas Caswell, Darol Chamberlain, Daniel R. Schuette, Hugh Philipp, Detlef M. Smilgies and Sol M. Gruner SAE paper 2006-01-1041, 2006
[15]Tonini S., Gavaises M., Arcoumanis ., Cossali G.E., Marengo M., paper 06-06-239, ICLASS Kyoto, Japan, 2006
[16]Wigley G., Mehdi M.,Williams M., Pitcher G. and Helie J., Paper ID ICLASS06-075, Kyoto 2006
[17] Van Romunde Z., Aleiferis P.G., Atomization and Sprays 19, 1-39, 2009
[18]Zigan L., Schmitz I., Wensing M. and Leipertz A., ILASS 2010

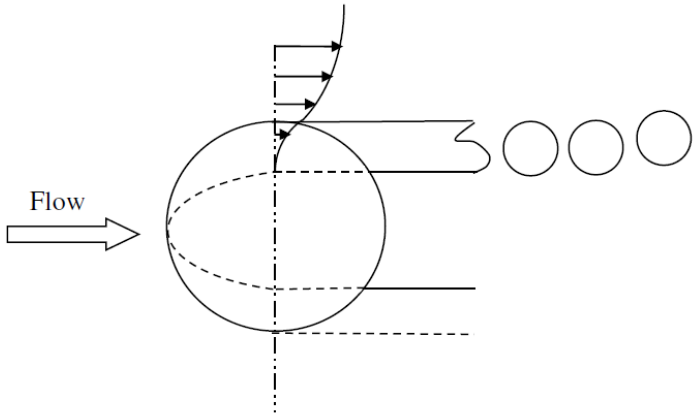

Figure 1. Boundary layer stripping of a droplet.

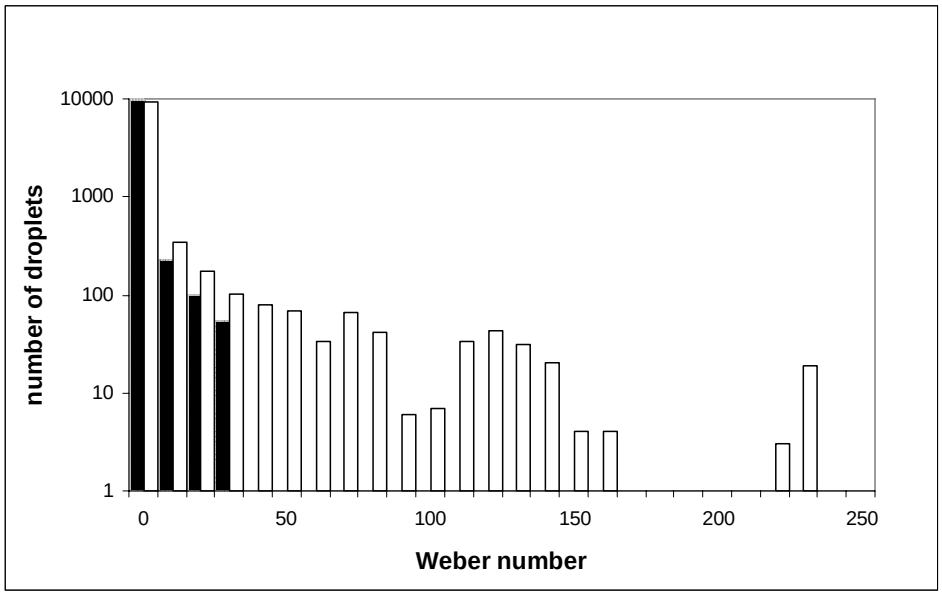

Figure 2. Droplet Weber number distribution at t=0.6ms. Case comment in the text.

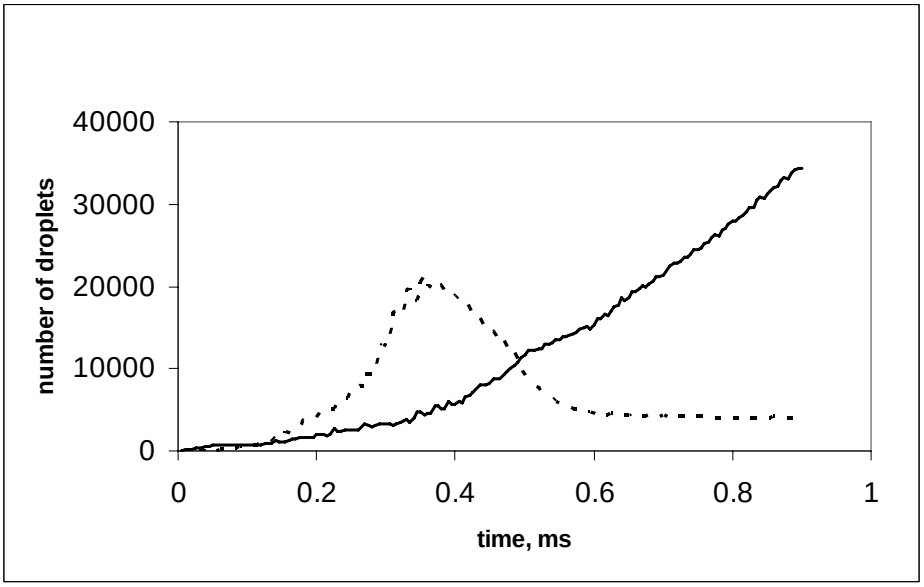

Figure 3. Occurrence of the different break-up regimes for the high Weber number case. Continuous line: Wave. Dashed line: Tab.

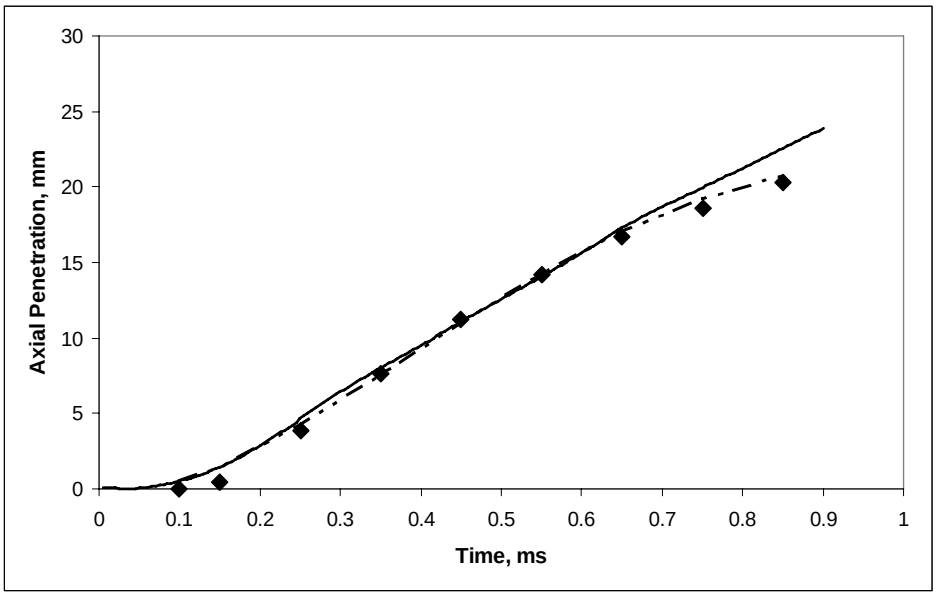

Figure 4. Axial Penetration versus time. Dot symbol: experimental. Continuous line: wave. Dotted line: hybrid model.

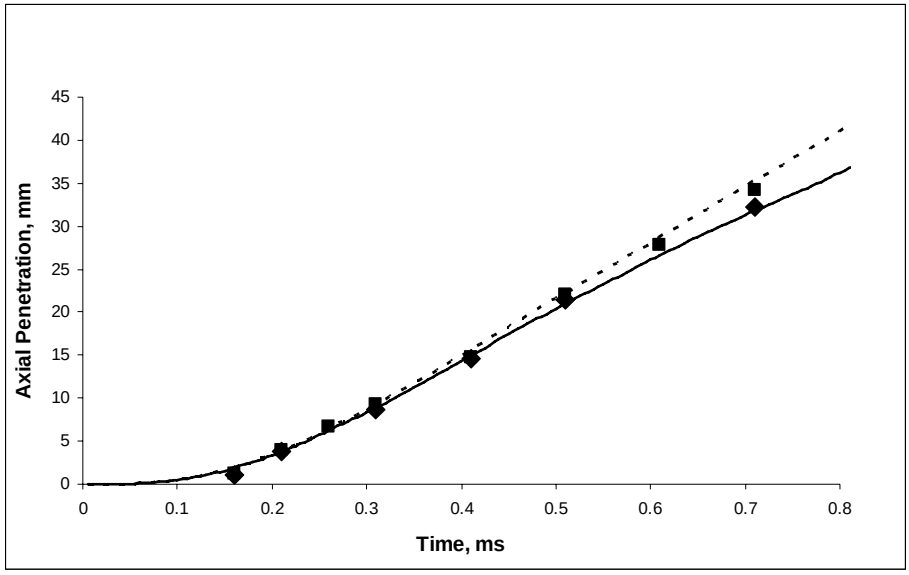

Figure 5 – Experimental and numerical Penetration for 2 different counter-pressures : 1bar (dashed line) and 2bar (continuous line); 200bar FUP; 60°C chamber temperature. 60°CA injector - non evaporating spray

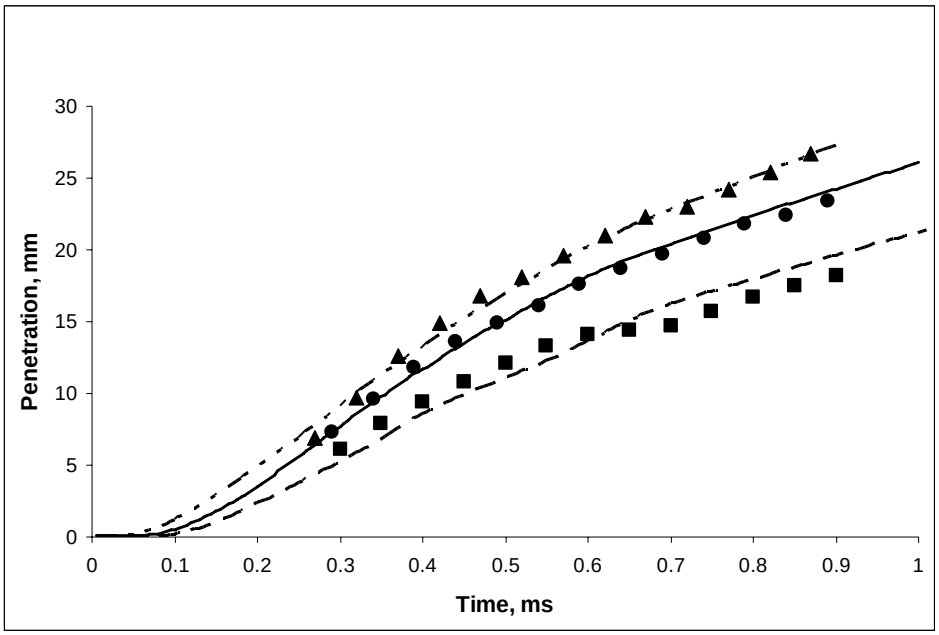

Figure 6 - Penetrations for Fuel Pressure variation; 10bar Counter pressure. 90°CA injector – evaporating spray. Lines: numerical, symbol: experimental. Triangles and dot-dashed line : 150 fuel pressure. Circle and continuous line: 100bar. Square and dashed line : 50bar.

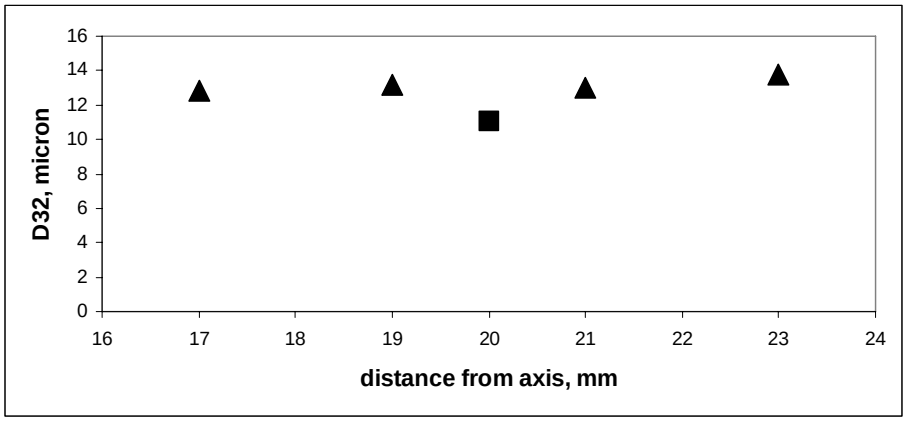

Figure 7 – Sauter Mean Diameter versus distance from the nozzle for numerical and the experimental result at 20mm distance. 120 bar fuel pressure, ambient conditions (1bar, 20°C).

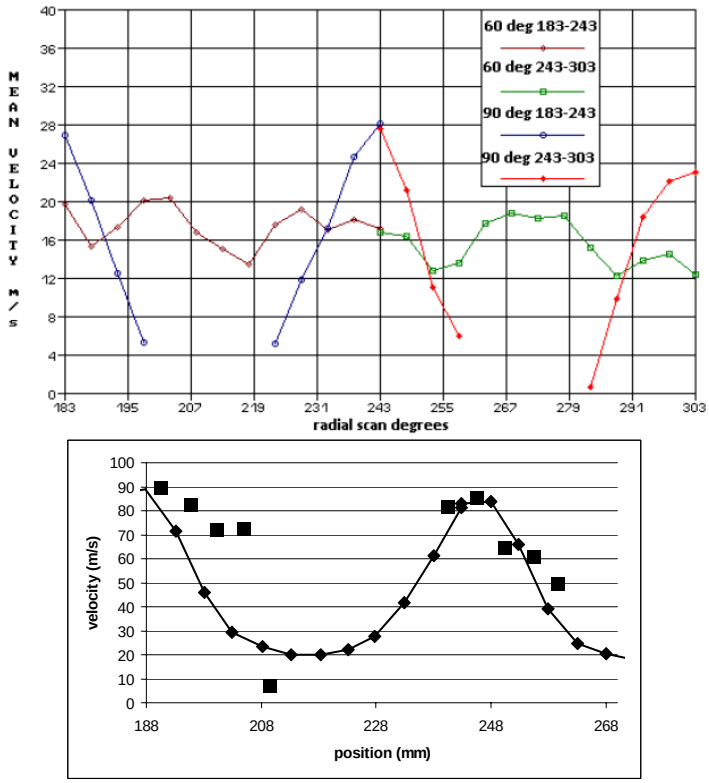

Figure 8: Top: Radial scan at 40mm below. Radial velocity profiles across three jets
60deg spray angle injector (dark red, green) and 90deg spray angle injector (blue, light red).
Bottom: Radial scan at 20mm below nozzle - axial velocity across 2 plumes with the 90° cone angle injector
Square: simulation, Diamond: measurements
All cases 120 bar fuel pressure, ambient conditions (1bar, 20°C).

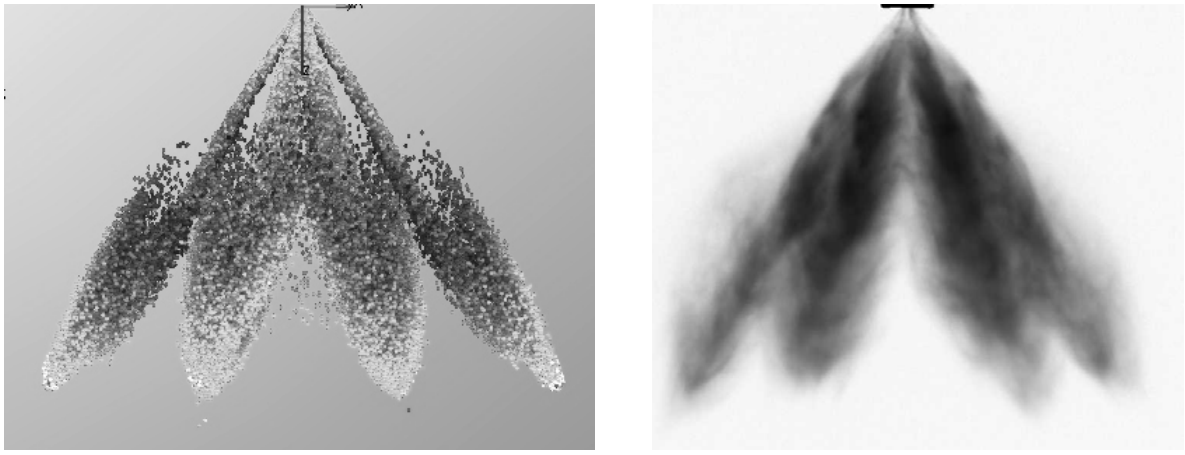

Figure 9. Example of interaction between two jets of a 60° MSI injector, XL3 version. Left: simulation; right: Imaging.